Analytical solution of the transfer rate equations in $LiNbO_3:Er^{3+}/Yb^{3+}$

2000 J. Phys.: Condens. Matter 12 521

(http://iopscience.iop.org/0953-8984/12/4/310)

J. Phys.: Condens. Matter **12** (2000) 521–527. Printed in the UK PII: S0953-8984(00)05566-1

Analytical solution of the transfer rate equations in $LiNbO_3:Er^{3+}/Yb^{3+}$

E Cantelar and F Cussó

Departamento de Física de Materiales, C-IV, Universidad Autónoma de Madrid, 28049 Madrid, Spain

E-mail: `fernando.cusso@uam.es`

Received 28 June 1999, in final form 24 September 1999

Abstract. The temporal evolution of the energy transfer between Yb^{3+} and Er^{3+} ions in lithium niobate ($LiNbO_3$), after selective ytterbium pulsed excitation, is investigated. The numerical integration of the rate equations shows that the temporal behaviour of the energy transfer between the two ions can be split into two stages: a first one dominated by transfer from Yb^{3+} to Er^{3+}, followed by another characterized by an equilibrium between transfer and back-transfer processes. In this last stage, it is possible to deduce an analytical expression for the relative population and the lifetime of the resonant manifolds, $^4I_{11/2}$ (Er^{3+}) and $^2F_{5/2}$ (Yb^{3+}). An excellent accordance between calculated lifetimes and those obtained experimentally (after excitation at 920 nm) in samples with different rare-earth concentrations has been observed.

1. Introduction

The energy transfer between Yb^{3+} and Er^{3+} in lithium niobate ($LiNbO_3$) has been recently studied under CW excitation [1]. It has been found that the energy transfer between both rare-earth ions could be described using a rate equation formalism with a macroscopic transfer coefficients equal to 2.4×10^{-16} and 1.8×10^{-16} cm^3 s^{-1}, for the transfer ($Yb^{3+} \rightarrow Er^{3+}$) and back-transfer ($Er^{3+} \rightarrow Yb^{3+}$) respectively. This efficient energy transfer from Yb^{3+} to Er^{3+} in $LiNbO_3$ makes it possible to reach population inversion in the $^4I_{13/2}$ erbium metastable level (upper laser level at 1.5 μm) at sufficiently low pumping levels.

Pulsed excitation measurements and the corresponding emission lifetimes can also be described using this formalism with the macroscopic transfer coefficients previously determined by CW excitation [2].

The temporal behaviour of the energy transfer can be further explored by numerical integration of the rate equations. In this way it is possible to improve the understanding of the underlying processes of the energy transfer and facilitate further exploitation of the potentialities of this description.

In this work, the temporal evolution of the energy transfer between Yb^{3+} and Er^{3+} ions in lithium niobate, under selective ytterbium excitation, is theoretically investigated. The results show that the energy transfer could be split in two different stages: a first one in which a rapid decay of the ytterbium ions takes place, followed by a second stage characterized by a parallel evolution of the population of erbium and ytterbium resonant energy levels ($^4I_{11/2}$ and $^2F_{5/2}$). In this last stage an analytical expression for the relative populations and lifetime of these manifolds has been obtained. The predicted lifetimes and the rare-earth

0953-8984/00/040521+07$30.00

concentration dependence are in excellent agreement with experimental data obtained under selective ytterbium pulsed excitation at 920 nm.

2. Experiment

Single crystals of Er^{3+} and Yb^{3+} co-doped $LiNbO_3$ have been grown by the Czochralski method with automatic diameter control by a crucible weighing system [3]. The starting materials were congruent $LiNbO_3$ and erbium and ytterbium oxides. The crystals have a fixed Er^{3+} concentration (0.5 mol%) and five different Yb^{3+} concentrations (0.1, 0.5, 1.0, 1.5 and 2.0 mol%) in the melt.

Lifetime measurements were obtained at room temperature around 1060 nm (${}^2F_{5/2} \rightarrow {}^2F_{7/2}$ ytterbium transition), under pulsed excitation around 920 nm using an optical parameter oscillator (Spectra Physics model MOPO-730). The fluorescence was analysed through an ARC monochromator model SpectraPro 500-i and then detected synchronously with an InGaAs photodiode and recorded by a digital oscilloscope. Geometry for luminescence collection has been cared in order to avoid radiation trapping effects that would generate a lengthening in the lifetime measurements [4].

3. Results and discussion

3.1. General spectroscopic properties

Figure 1(a) shows the un-polarized absorption spectra of an erbium singly doped lithium niobate sample ($[Er^{3+}] = 0.5$ mol%, dotted line) and a co-doped sample ($[Er^{3+}] = 0.5$ mol% and $[Yb^{3+}] = 1.0$ mol%, continuous line) in the 1 μm region. In the singly doped crystal the absorption spectrum corresponds to the ${}^4I_{15/2} \rightarrow {}^4I_{11/2}$ transition of erbium ions [5, 6], while in the co-doped crystal the absorption corresponds to the superposition of this transition plus the ${}^2F_{7/2} \rightarrow {}^2F_{5/2}$ transition of ytterbium ions [7–9]. In this figure it is apparent that ytterbium sensitization improves the excitation of Er^{3+}-doped $LiNbO_3$, providing a broader and more intense absorption band suitable for laser diode excitation.

Although the ${}^2F_{5/2}$ (Yb^{3+}) and ${}^4I_{11/2}$ (Er^{3+}) multiplets overlap in a wide spectral range (960–1000 nm) it is possible to excite selectively the ytterbium ions in the range 875–960 nm (see figure 1(a)). After excitation at 920 nm, figure 1(b), the excited ytterbium ions may relax radiatively to their ground state, ${}^2F_{7/2}$, giving luminescence in the range 920–1100 nm, or transfer to the ${}^4I_{11/2}$ erbium level, according to the cross relaxation mechanism: ${}^2F_{5/2} \rightarrow {}^2F_{7/2}(Yb^{3+})$:${}^4I_{15/2} \rightarrow {}^4I_{11/2}(Er^{3+})$ characterized by a macroscopic transfer coefficient C_{25} [1].

From the ${}^4I_{11/2}$ erbium multiplet, the excitation can be transferred back to the ytterbium ions by the inverse cross relaxation process, characterized by a macroscopic back-transfer coefficient C_{52}, or relax within the Er^{3+} ions. This relaxation produces luminescence in the 1.0 μm region, corresponding to the ${}^4I_{11/2} \rightarrow {}^4I_{15/2}$ transition, and in the 1.5 μm region, corresponding to the ${}^4I_{13/2} \rightarrow {}^4I_{15/2}$ transition (the erbium metastable level, ${}^4I_{13/2}$, is populated via non-radiative connection from the upper level) [5, 6].

According to the standard description of the Er^{3+}/Yb^{3+} co-doped materials the transfer of a second photon from ytterbium to one excited erbium generates infrared to visible energy up-conversion [10–12] through the cross relaxation process ${}^2F_{5/2} \rightarrow {}^2F_{7/2}(Yb^{3+})$:${}^4I_{11/2} \rightarrow {}^4F_{7/2}(Er^{3+})$. The erbium ions excited to the ${}^4F_{7/2}$ level relax non-radiatively to the ${}^4S_{3/2}$ level, from where the de-excitation is partially radiative to the ground state (green emission in the region 520–580 nm) and partially non-radiative to the ${}^4I_{11/2}$ level. In lithium niobate

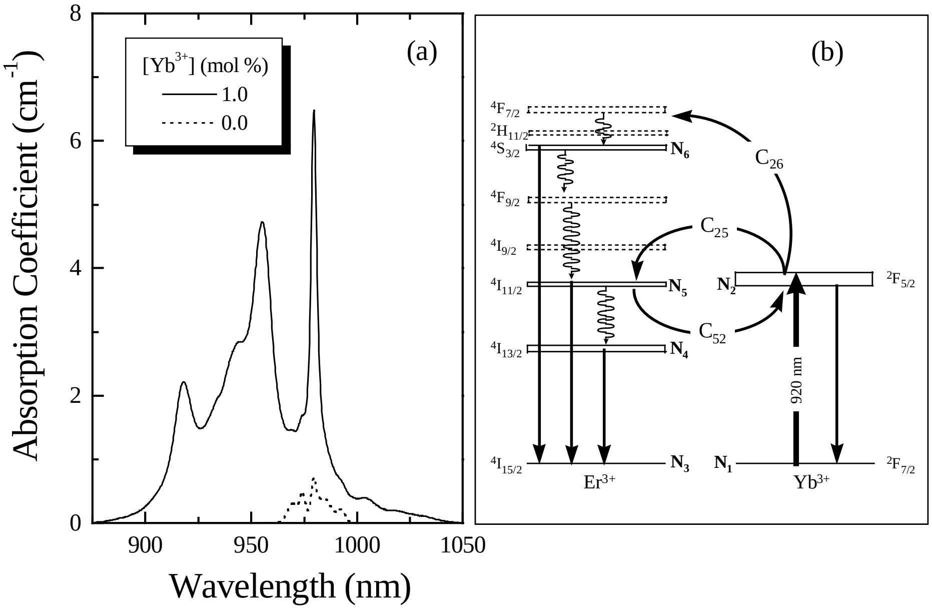

Figure 1. (a) Un-polarized absorption spectra in the 880–1050 nm region for a co-doped sample, [Er^{3+}] = 0.5 mol%, [Yb^{3+}] = 1.0 mol% (solid line), and for an erbium doped sample (0.5 mol%, dotted line). (b) Schematic energy level diagram of LiNbO$_3$:Er^{3+}/Yb^{3+} showing the multiplets involved in the energy transfer processes as well as the dominant emissions.

the intermediate levels (^{4}F$_{9/2}$ and ^{4}I$_{9/2}$) experience a fast non-radiative decay so that their populations and contributions to luminescence can be ignored [5, 6].

Although in some materials this up-conversion mechanism is highly efficient, allowing up-conversion laser generation [13], in LiNbO$_3$:Er^{3+} the ^{4}S$_{3/2}$ level has a relatively low quantum efficiency of approximately 0.2 [14], and there is a relevant non-radiative relaxation back to the ^{4}I$_{11/2}$ level.

3.2. Rate equations

The transfer dynamics between Er^{3+} and Yb^{3+} ions, sketched in figure 1(b), can be described using the rate equation formalism [1, 2], which is summarized by the following rate equations:

$$\frac{\mathrm{d}N_2}{\mathrm{d}t} = \sigma_{Yb}\phi N_1 - (A_{21} + W_{21}^{NR})N_2 - C_{25}N_2N_3 + C_{52}N_5N_1 - C_{26}N_2N_5 \tag{1}$$

$$\frac{\mathrm{d}N_4}{\mathrm{d}t} = (A_{54} + W_{54}^{NR})N_5 + A_{64}N_6 - (A_{43} + W_{43}^{NR})N_4 \tag{2}$$

$$\frac{\mathrm{d}N_5}{\mathrm{d}t} = (A_{65} + W_{65}^{NR})N_6 + C_{25}N_2N_3 - C_{52}N_5N_1 - C_{26}N_2N_5 - (A_{54} + A_{53} + W_{54}^{NR})N_5 \tag{3}$$

$$\frac{\mathrm{d}N_6}{\mathrm{d}t} = C_{26}N_2N_5 - (A_{65} + A_{64} + A_{63} + W_{65}^{NR})N_6 \tag{4}$$

$$N_3 + N_4 + N_5 + N_6 = N_{Er} \tag{5}$$

$$N_1 + N_2 = N_{Yb} \tag{6}$$

where N_i is the population density of the ith-level, A_{ij} and W_{ij}^{NR} the radiative and non-radiative transition probabilities between the i and j states, σ_{Yb} is the Yb^{3+} absorption cross section at

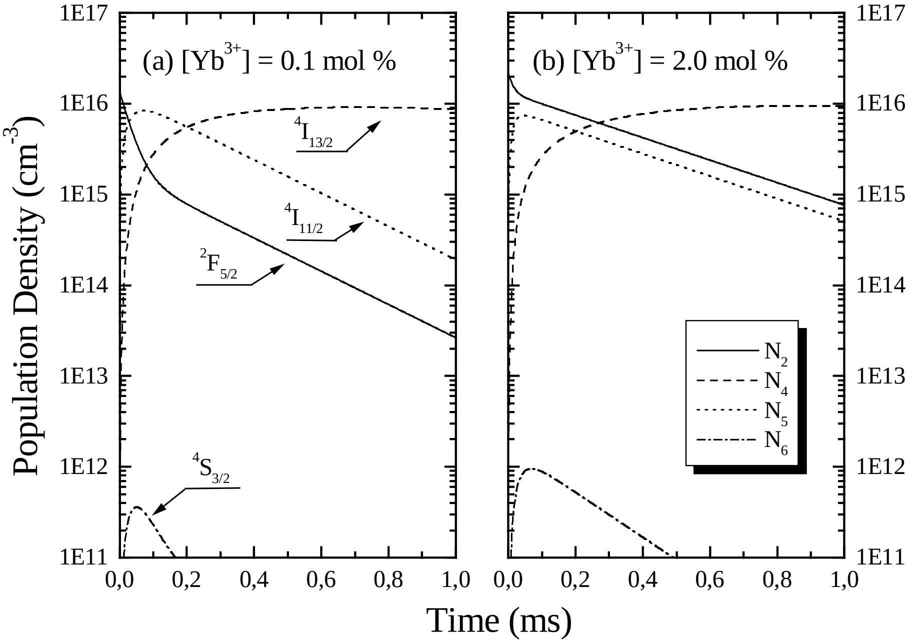

Figure 2. Temporal evolution (in a logarithmic scale) of the population densities after selective ytterbium pulsed excitation obtained by numerical integration of equations (1)–(6) in two co-doped samples with the same erbium concentration (0.5 mol%) and different ytterbium concentrations: (a) [Yb^{3+}] = 0.1 mol% and (b) [Yb^{3+}] = 2.0 mol%.

the pumping wavelength, ϕ is the pumping flux and finally C_{25}, C_{52} and C_{26} are coefficients (in units of cm^3 s^{-1}) which quantify the energy transfer, the back-transfer and the up-conversion processes respectively.

The spectroscopic parameters (transition probabilities) of Er^{3+} and Yb^{3+} in LiNbO$_3$ are reported in the literature [5–9], and the transfer and back-transfer coefficients (C_{25} and C_{52}) have been previously determined for the system LiNbO$_3$:Er^{3+}/Yb^{3+} under CW experiments ($C_{25} = 2.4 \times 10^{-16}$ cm^3 s^{-1} and $C_{52} = 1.8 \times 10^{-16}$ cm^3 s^{-1}) [1]. The remaining transfer coefficient, C_{26}, describes the cross relaxation process ^{2}F$_{5/2}$ → ^{2}F$_{7/2}$(Yb^{3+}):^{4}I$_{11/2}$ → ^{4}F$_{7/2}$(Er^{3+}) and therefore the difference from C_{25} is related to the different excitation process within the Er^{3+} ions. Considering that the ratio between the electric dipole strengths of the ^{4}I$_{11/2}$ → ^{4}F$_{7/2}$ and ^{4}I$_{15/2}$ → ^{4}I$_{11/2}$ transitions of erbium ions is approximately a factor of 2 [5, 6], it has been assumed that $C_{26} \approx 2C_{25} = 4.8 \times 10^{-16}$ cm^3 s^{-1}.

Using the model described by equations (1)–(6), the temporal evolution of the energy transfer processes after pulsed excitation can be explored. In order to do that, the initial conditions assumed to integrate equations (1)–(6) are such that they reproduce the experimental conditions used in our experiments. In this way, an excitation pulse (10 ns duration) of 20 mJ at 920 nm ($N_{ph} = 9 \times 10^{16}$ photons) incident on $d = 1$ mm thick samples with N_{Yb} ions cm^{-3}, with an absorption cross section at that wavelength $\sigma_{Yb}(920\,\text{nm}) = 7.96 \times 10^{-21}$ cm^2, produces the initial excitation of $N_2(0) = N_{ph}(1 - \exp(-\sigma_{Yb} d N_{Yb}))$ Yb ions cm^{-3}. The initial ground state Yb^{3+} population is therefore $N_1(0) = N_{Yb} - N_2(0)$. All the Er^{3+} ions are considered initially (prior to energy transfer) in the ground state ($N_3(0) = N_{Er} = 1.13 \times 10^{20}$ ions cm^{-3}) and $N_4(0) = N_5(0) = N_6(0) = 0$. Using these starting conditions and assuming that after

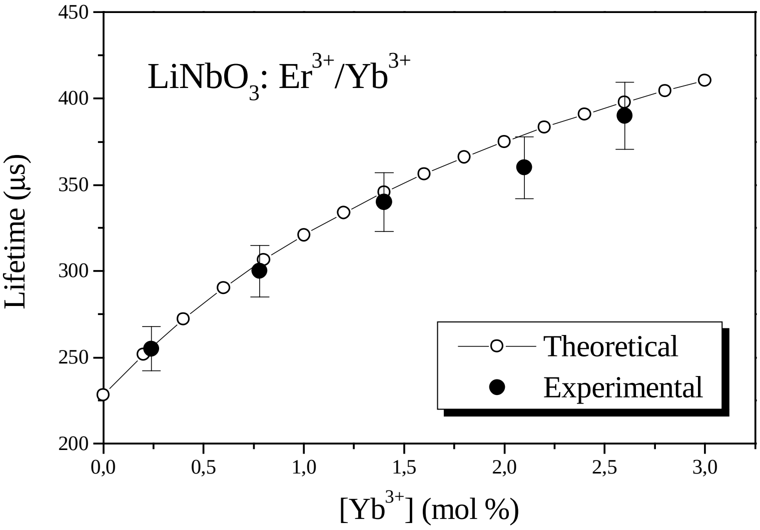

Figure 3. Comparison between the $^2F_{5/2}$ (Yb^{3+}) lifetime predicted by equation (10), open circles, and measured in co-doped samples, solid circles. The erbium concentration was always the same (0.75 mol%) while ytterbium concentration was variable (0.24, 0.78, 1.4, 2.1 and 2.6 mol%).

the initial pulse the excitation is set equal to zero ($\phi = 0$) equations (1)–(6) are numerically integrated.

Figure 2 shows the temporal evolution of the principal population densities of erbium and ytterbium excited states ($^4I_{13/2}$, $^4I_{11/2}$, $^4S_{3/2}$ and $^2F_{5/2}$). Figure 2(a) corresponds to samples with low ytterbium concentration (0.1 mol% or $N_{Yb} = 2.1 \times 10^{19}$ ions cm^{-3}) while figure 2(b) corresponds to the higher doping level (2.0 mol% or $N_{Yb} = 5.0 \times 10^{20}$ ions cm^{-3}). All the samples have the same erbium concentration ($N_{Er} = 1.13 \times 10^{20}$ ions cm^{-3}).

It can be observed that the energy transfer between Er^{3+} and Yb^{3+} could be split into two different stages. A first one, where transfer from Yb^{3+} to Er^{3+} dominates, produces a fast change in the population of the excited multiplets. It can be observed that the population of the $^2F_{5/2}$ (Yb^{3+}) excited state decreases while the Er^{3+} excited states are populated.

The second stage is characterized by a dynamical equilibrium between population densities of the resonant levels ($^4I_{11/2}$ (Er^{3+}) and $^2F_{5/2}$ (Yb^{3+})). From that point onwards a parallel temporal evolution in the population densities of both multiplets takes place:

$$\mathrm{d}N_2/\mathrm{d}t = \mathrm{d}N_5/\mathrm{d}t.$$

Considering that the population in the upper erbium level ($^4S_{3/2}$) is negligible (see figure 2), we assume in the following $N_6 = 0$. Furthermore, taking into account that the excited state populations ($<10^{16}$ ions cm^{-3}) are a small fraction of the Er^{3+} or Yb^{3+} ions (N_{Er}, $N_{Yb} > 10^{19}$ ions cm^{-3}), it can be assumed that $N_3 \approx N_{Er}$ and $N_1 \approx N_{Yb}$. Both considerations allow us to obtain, from equations (1) and (3), that:

$$\frac{N_2(t)}{N_5(t)} = \frac{A_{5m} + 2C_{52}N_{Yb}}{A_{2m} + 2C_{25}N_{Er}} \tag{7}$$

where $A_{2m} = A_{21} + W_{21}^{NR} = 1.72 \times 10^3$ s^{-1} [8] and $A_{5m} = \sum_{j=3,4} A_{5j} + W_{54}^{NR} = 4.55 \times 10^3$ s^{-1} [5].

This expression indicates that the ratio N_2/N_5 reaches a constant value which depends on the decay rates of these excited states (A_{2m}, A_{5m}), the transfer coefficients (C_{25}, C_{52}) and the rare-earth concentrations. Changing the relative concentration ($[\mathrm{Yb}^{3+}]/[\mathrm{Er}^{3+}]$) within the solubility limits in lithium niobate [3], the ratio N_2/N_5 changes substantially. For instance, as can be noted comparing figures 2(a) and 2(b), this ratio changes from 0.14 to 1.50 in samples co-doped with 0.5 mol% of Er^{3+} and 0.1 or 2.0 mol% of Yb^{3+} respectively; i.e. the dominant excited state population corresponds to $\mathrm{Er}^{3+}(^4\mathrm{I}_{11/2})$ or $\mathrm{Yb}^{3+}(^2\mathrm{F}_{5/2})$ respectively.

3.3. Analytical expression for the $^4I_{11/2}(Er^{3+})$ and $^2F_{5/2}(Yb^{3+})$ lifetimes

As a consequence of the dynamical equilibrium between the $^4\mathrm{I}_{11/2}(\mathrm{Er}^{3+})$ and $^2\mathrm{F}_{5/2}(\mathrm{Yb}^{3+})$ excited states, both manifolds decay with the same lifetime, $\tau(\mathrm{Er/Yb})$. In fact, the total transition probability can be calculated as the statistically averaged de-excitation probability of each multiplet weighted by the population density of each one; that is:

$$[\tau(\mathrm{Er/Yb})]^{-1} = \left[\frac{N_2}{N_2+N_5}\right] A_{2m} + \left[\frac{N_5}{N_2+N_5}\right] A_{5m} = \frac{(N_2/N_5)A_{2m} + A_{5m}}{1+(N_2/N_5)} \tag{8}$$

which, taking into account equation (7), can be re-written as:

$$\tau(\mathrm{Er/Yb}) = \frac{1+[(A_{5m}+2C_{52}N_{Yb})/(A_{2m}+2C_{25}N_{Er})]}{A_{5m}+A_{2m}[(A_{5m}+2C_{52}N_{Yb})/(A_{2m}+2C_{25}N_{Er})]}. \tag{9}$$

Figure 3 shows the comparison between the lifetime values calculated (open circles) from equation (9) and those obtained experimentally (solid circles) in samples from the different crystal boules, having crystal concentrations of: 0.75 mol% erbium and 0.24, 0.78, 1.4, 2.1 and 2.6 mol% ytterbium. As can be observed in the figure, there is an excellent agreement between the experimental values and those calculated from equation (9).

We may therefore conclude that the temporal evolution of the energy transfer in $\mathrm{LiNbO_3}$:$\mathrm{Er}^{3+}/\mathrm{Yb}^{3+}$ is adequately described using the rate equation formalism. Exploring the consequences of this model, the numerical integration of the rate equations shows that the energy transfer process could be split into two different stages. The first one dominated by the energy transfer from Yb^{3+} to Er^{3+}, followed by another stage of dynamical equilibrium between the populations of $^4\mathrm{I}_{11/2}$ and $^2\mathrm{F}_{5/2}$ erbium and ytterbium excited multiplets. This equilibrium is reached some tens of microseconds after excitation, with a slight dependence on the rare-earth concentration, and then a parallel temporal evolution in the population of both manifolds is observed. The relative populations, $N_2(t)/N_5(t)$, as well as the common decay lifetime can be calculated straightforwardly using expressions (7) and (9), the spectroscopic parameters [5–9], the macroscopic transfer coefficients [1] and the rare-earth concentrations.

These analytical solutions may simplify the calculations required to model optical amplifiers or lasers using $\mathrm{Er}^{3+}/\mathrm{Yb}^{3+}$ co-doped $\mathrm{LiNbO_3}$, where the population of the excited states should be evaluated to analyse the pump and signal evolution through the amplifying medium [15–17].

Acknowledgments

This work is partially supported by CICYT (PB97-0019) and Comunidad de Madrid (07T/0026/1998).

References

[1] Cantelar E, Muñoz J A, Sanz-García J A and Cussó F 1998 *J. Phys.: Condens. Matter* **10** 8893
[2] Cantelar E and Cussó F 1999 *Appl. Phys.* B **69** 29
[3] Cantelar E, Sanz-García J A and Cussó F 1999 *J. Cryst. Growth* **205** 196

[4] Muñoz J A, Herreros B, Lifante G and Cussó F 1998 *Phys. Status Solidi* a **168** 525

[5] Núñez L, Lifante G and Cussó F 1996 *Appl. Phys.* B **62** 485

[6] Amin J, Dussardier B, Schweizer T and Hempstead M 1996 *J. Lumin.* **69** 17

[7] Jones J K, de Sandro J P, Hempstead M, Shepherd D P, Large A C, Tropper A C and Wilkinson J S 1995 *Opt. Lett.* **20** 1477

[8] Huang C and McCaughan L 1997 *IEEE Photon. Technol. Lett.* **9** 599

[9] Montoya E, Lorenzo A and Bausá L E 1999 *J. Phys.: Condens. Matter* **11** 311

[10] Johnson L F, Guggenheim H J, Rich T C and Ostermayer F W 1972 *J. Appl. Phys.* **43** 1152

[11] Zandi B, Merkle L D, Hutchinson J A, Verdun H R and Chai B H T 1994 *J. Physique Coll.* IV C4 587

[12] Simondi-Teisseire B, Viana B, Vivien D and Lejus A M 1996 *Opt. Mater.* **6** 267

[13] Möbert P E A, Heumann E and Huber G 1997 *Opt. Lett.* **22** 1412

[14] Muñoz J A, Di Paolo R E, Duchowicz R, Tocho J O and Cussó F 1998 *Solid State Commun.* **107** 487

[15] Dinand M and Sohler W 1994 *IEEE J. Quantum Electron.* **30** 1267

[16] Bandelloni G, Beretta C and Montrosset I 1999 *Proc. 9th Eur. Conf. on Integrated Optics, ECIO'99 (Torino, 1999)* pp 301–4

[17] Dierov V, Kutsenko A B, Sandmann C, Tallian F and von der Osten W 1999 *Appl. Phys.* B **68** 767